

See discussions, stats, and author profiles for this publication at: <https://www.researchgate.net/publication/316157182>

Aromatase inhibitors and apoptotic inducers: Design, synthesis, anticancer activity and molecular modeling studies of novel...

Article in *European Journal of Medicinal Chemistry* · April 2017

DOI: 10.1016/j.ejmech.2017.04.028

CITATION

1

READS

82

7 authors, including:



Mostafa Ghorab

college of pharmacy,king saud univeristy

236 PUBLICATIONS 2,493 CITATIONS

SEE PROFILE



Aiten M. Soliman

Egyptian Atomic Energy Authority

14 PUBLICATIONS 29 CITATIONS

SEE PROFILE



Dalal abou el ella

Ain Shams University

56 PUBLICATIONS 402 CITATIONS

SEE PROFILE

Some of the authors of this publication are also working on these related projects:



Evaluation of the anticancer activity of synthesized compounds or semi-synthesized natural products against different cancer cell lines and normal cells [View project](#)



Research paper

Aromatase inhibitors and apoptotic inducers: Design, synthesis, anticancer activity and molecular modeling studies of novel phenothiazine derivatives carrying sulfonamide moiety as hybrid molecules



Mostafa M. Ghorab^{a, b, *}, Mansour S. Alsaid^a, Nermin Samir^c, Ghada A. Abdel-Latif^d, Aiten M. Soliman^b, Fatma A. Ragab^e, Dalal A. Abou El Ella^{c, f}

^a Department of Pharmacognosy, College of Pharmacy, King Saud University, P.O. Box 2457, Riyadh 11451, Saudi Arabia

^b Department of Drug Radiation Research, National Center for Radiation Research and Technology, Egyptian Atomic Energy Authority, Cairo 113701, Egypt

^c Department of Pharmaceutical Chemistry, Faculty of Pharmacy, Ain Shams University, Cairo 11566, Egypt

^d Department of Pharmacology, Faculty of Pharmacy, Misr International University, Cairo, Egypt

^e Department of Pharmaceutical Chemistry, Faculty of Pharmacy, Cairo University, Cairo, Egypt

^f Faculty of Pharmacy, Nahda University, 62511 New Beni Suef (NUB), Egypt

ARTICLE INFO

Article history:

Received 7 February 2017

Received in revised form

10 April 2017

Accepted 12 April 2017

Available online 15 April 2017

Keywords:

Phenothiazine

Benzenesulfonamide

Anticancer

Aromatase inhibitors

Apoptosis

ABSTRACT

Hybrid molecules are used as anticancer agents to improve effectiveness and diminish drug resistance. So, the current study aimed to introduce twenty novel phenothiazine sulfonamide hybrids **5–22**, **24** and **25** of promising anticancer activity. Compounds **11** and **13** revealed more potent anticancer properties (IC₅₀ 8.1 and 8.8 μM) than that of the reference drug (doxorubicin, IC₅₀ = 9.8 μM) against human breast cancer cell line (T47D). To determine the mechanism of their anticancer activity, compounds **5**, **6**, **7**, **11**, **13**, **14**, **16**, **17**, **19** and **22** that showed promising activity on T47D, were evaluated for their aromatase inhibitory effect. The study results disclose that the most potent aromatase inhibitors **11** and **13** showed the lowest IC₅₀ (5.67 μM and 6.7 μM), respectively on the target enzyme. Accordingly, the apoptotic effect of the most potent compound **11** was extensively investigated and showed a marked increase in Bax level up to 55,000 folds, and down-regulation in Bcl2 to 5.24*10⁻⁴ folds, in comparison to the control. Furthermore, the effect of compound **11** on caspases 3, 8 and 9 was evaluated and was found to increase their levels by 20, 34, and 8.9 folds, respectively, which indicates the activation of both intrinsic and extrinsic pathways. Also, the effect of compound **11** on the cell cycle and its cytotoxic effect were examined. Moreover, a molecular docking and computer aided ADMET studies were adopted to confirm their mechanism of action.

© 2017 Elsevier Masson SAS. All rights reserved.

1. Introduction

Apoptosis is a programmed “self-automated” cell death with caspase-3 as a key player in apoptotic process execution [1]. It is critical for the homeostasis that conserves cellular integrity. Impairment of apoptosis signaling pathways may lead to several diseases including cancer [2]. Depending on the apoptogenic

mechanisms of aromatase inhibitors [3,4], the inhibition of aromatase enzyme plays an important strategy in the treatment of cancer. Aromatase is responsible for a key step in the biosynthesis of estrogens from androgens by aromatization [5]. High levels of estrogens stimulate the hormone-dependent breast cancer progression and metastasis in both pre- and postmenopausal women [6]. Therefore, targeting critical apoptosis regulators with a goal of apoptosis induction in cancer cells and suppression of estrogen biosynthesis by aromatase inhibition is an attractive approach for the treatment of hormone-sensitive breast cancer [4,7,8]. Aromatase can be competitively inhibited by various classes of steroidal and non-steroidal compounds [9]. Novel potent, more selective, and less toxic aromatase inhibitors (AIs) are necessary due to the

* Corresponding author. Department of Pharmacognosy, College of Pharmacy, King Saud University, P.O. Box 2457, Riyadh 11451, Saudi Arabia.

E-mail addresses: mmsghorab@yahoo.com, mghorab@ksu.edu.sa (M.M. Ghorab).

side effects evolved from the prolonged use of them [10].

In our previous work [11], we synthesized a novel series of chromene sulfonamide hybrids based on structural diversification of a lead compound (A) (Fig. 1) revealed by Pingaew *et al* in 2015 that proved to have potent aromatase inhibitory activity ($IC_{50} = 0.2 \mu M$) [12]. Where compound (B) methoxypyrimidinyl derivative of chromene benzenesulfonamide (Fig. 1) showed significant anticancer activity ($IC_{50} = 8.8 \mu M$) higher than that of

doxorubicin ($IC_{50} = 9.8 \mu M$) against human breast cancer cell line (T47D). Also, it demonstrated the inhibitory effect on the aromatase enzyme with $IC_{50} = 4.6 \mu M$ and induced the levels of active caspase 3, caspase 8 and caspase 9. Moreover, it surprisingly boosted the Bax/Bcl2 ratio 5936 & 33,000 folds, respectively compared to the control. In addition, the molecular docking study of compound (B) revealed that it formed a significant H-bond between its sulfonyl oxygen and Met 374 the essential amino acid for the inhibitory

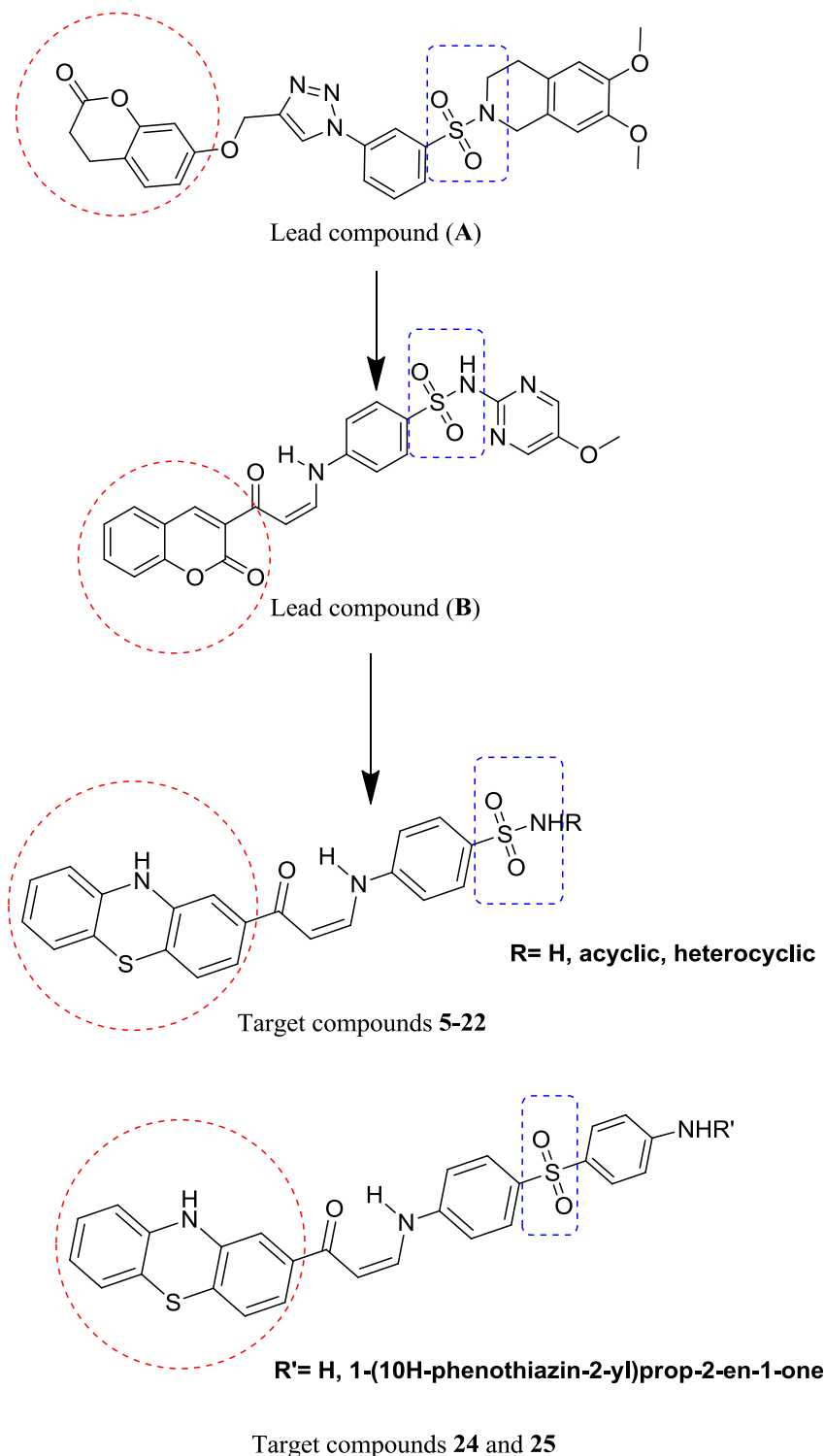


Fig. 1. Structure based design of phenthiazine derivatives 5–22, 24 and 25 as AIs.

activity and interacts with a large hydrophobic pocket (Cys 437, Ala 306, and Ala 307) through its coumarinyl moiety [11]. As a continuation of our previous work [13,14], we attempted to produce another novel AIs using both compounds (A) and (B) as leads. So, new analogs designed preserving the sulfonamide moiety **5–22** or sulfonyl **24** and **25** (blue dotted quadrant) and replacing coumarin ring with larger phenothiazine one (red dotted circle) to accommodate the large hydrophobic pocket present in the enzyme (Fig. 1). To prove our concept, we compared the binding mode of lead compound (B) with that of our newly designed series and the results revealed that both have the same binding mode with the aromatase enzyme as shown in Fig. 2.

2. Results and discussion

2.1. Chemistry

In this work, a novel series of phenothiazine derivatives carrying benzenesulfonamide was synthesized. Thus, interaction of 1-(10H-phenothiazin-2-yl) ethanone **1** with dimethylformamide-dimethyl acetal (DMF-DMA) **2** under reflux in dry xylene gave the strategic starting material (*E*)-3-(dimethylamino)-1-(10H-phenothiazin-2-yl)-prop-en-1-one **3**. Enaminone **3** was assigned an *E*-configuration based on its ^1H NMR as the coupling constant of the doublet signals for olefinic protons is 12.5 Hz correlated to the *E*-isomers [15]. Enaminone **3** was reacted with sulfa drugs **4** and/or dapson **23** in absolute ethanol containing glacial acetic acid (2:1) [16], the corresponding phenothiazine-sulfonamide derivatives **5–22**, **24** and **25** (Schemes 2 and 3) were obtained. IR of **5–22** indicated the presence of characteristic bands for NH, CO and SO_2 groups. ^1H NMR of **5–22**, **24** and **25** supported that these structures in (*Z*) form, as the coupling constant of the doublet signal for olefinic protons equal to 10–10.5 Hz. *Z* form is stabilized by intramolecular hydrogen bonding (Scheme 1). ^1H NMR of **5–22** indicated the presence of two doublets at 5.7–6.4 ppm and 7.3–7.9 ppm assigned to $\text{CH}=\text{CH}$ and $\text{CH}-\text{NH}$, respectively, singlet at 8.1–8.9 ppm attributed to SO_2NH , singlet at 10.3–10.4 ppm due to NH phenothiazine and singlet at 10.5–11.9 ppm for NH group. ^{13}C NMR of **5–22** exhibited signals at 94.7–95.8 ppm for $\text{CH}=\text{CH}$, 142.5–146.7 ppm for $\text{CH}-\text{NH}$ and 185.1–189.5 ppm for CO group. In addition, the interaction of compound **3** with dapson **23** in a molar ratio (1:1 mol) gave the corresponding mono-substituted compound **24**, while the bis-compound **25** was obtained in the same condition but

in a molar ratio (2:1 mol) (Scheme 3). The IR of **24** revealed the presence of bands at 3356, 3213 cm^{-1} for (NH, NH_2), 1635 cm^{-1} for CO and 1363, 1197 cm^{-1} for SO_2 , while, IR of **25** showed bands at 3410, 3354 cm^{-1} for 4NH, 1635 cm^{-1} for 2CO groups and 1390, 1197 cm^{-1} for SO_2 . ^1H NMR of **24** revealed two doublets at 6.1 and 7.5 ppm for $\text{CH}=\text{CH}$ protons, singlet at 6.2 ppm assigned to NH_2 , singlet at 10.4 ppm for NH phenothiazine and singlet at 11.9 ppm attributed to NH group. ^{13}C NMR of **24** exhibited signals at 95.3, 144.8 ppm due to $\text{CH}=\text{CH}$ and 187.0 ppm for CO group. ^1H NMR of **25** revealed two doublets at 5.7 and 7.4 ppm due to $\text{CH}=\text{CH}$, singlet at 10.4 ppm for 2NH phenothiazine, singlet at 11.9 ppm attributed to 2NH groups. ^{13}C NMR of **25** exhibited signals at 95.3, 143.3 ppm for 2CH = CH and 185.1 for 2CO groups.

2.2. Biological activity

2.2.1. Anticancer activity against T47D human breast cancer cell line

The newly synthesized phenothiazine derivatives **3**, **5–22**, **24** and **25** were preliminarily screened for their *in vitro* cytotoxic activity against T47D human breast cancer cell line utilizing the Sulfo-Rhodamine-B (SRB) assay [17]. From the results obtained (Table 1), it is apparent that all the tested phenothiazines exerted anticancer activity with IC_{50} values ranging from 8.1 μM to 135.8 μM . Sulfonamide group plays a major role in the anticancer activity as apparent from comparing the IC_{50} value of compound **5** bearing unsubstituted sulfonamide and compound **3** bearing a terminal tertiary amine (IC_{50} = 67.6 μM , 135.8 μM), respectively.

Results showed that compounds **7**, **11**, **13** and **22** have significant anticancer activity (Table 1) with IC_{50} less than 25 μM . Among them compounds **11** with unsubstituted thiazolyl ring and **13** with unsubstituted pyridine exerted the highest activity having IC_{50} values of 8.1 and 8.8 μM , respectively which are more potent than that of the reference drug used, Doxorubicin (IC_{50} 9.8 μM).

2.2.2. Aromatase inhibitory activity

The aromatase inhibitory activity of the most potent compounds **5**, **6**, **7**, **11**, **13**, **14**, **16**, **17**, **19**, **22** and **24** was determined. Results showed that most of the tested compounds have moderate to high inhibitory activity ranging from 28.90% to 72.22%. Four compounds **7**, **11**, **13** and **22** showed percentage inhibition above 60% and their IC_{50} values were also recorded as 9.67, 5.67, 6.70 and 8.90 μM , respectively (Table 1). Compound **11** bearing unsubstituted thiazole ring showed the lowest IC_{50} value (5.67 μM), and 68.32% aromatase inhibition. Letrozole was used as a reference drug with (29.5 μM), and 58% aromatase inhibition.

2.2.3. Apoptosis studies

From the previous results, most of the synthesized phenothiazine-sulfonamide derivatives proved to have aromatase inhibitory activity. As mentioned before, the inhibition of aromatase enzyme leads consequently to the induction of apoptosis [3,4]. Therefore, to reveal the proapoptotic potential of our target compounds, compound **11** with the lowest IC_{50} (5.67 μM) on the aromatase enzyme was chosen to explore its ability to induce the apoptosis cascade.

2.2.3.1. Activation of proteolytic caspases cascade. Activation of caspases plays a key role in the initiation and execution of the apoptotic process [18]. Among the caspases, caspase-3, a vital player that cleaves multiple proteins in the cells, leading to apoptotic cell death [1]. The effect of compound **9** on caspase 3 was evaluated and compared to vandetanib as a reference drug. It showed an increase in the level of active caspase 3 by 7 folds, compared to the control cells, and induced caspase 3 approximately

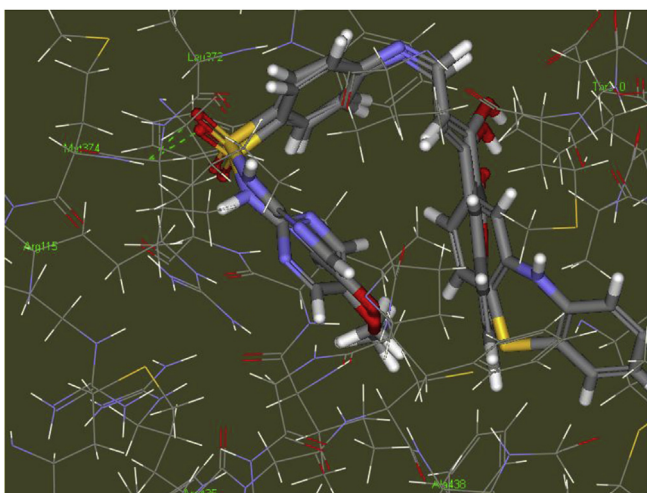
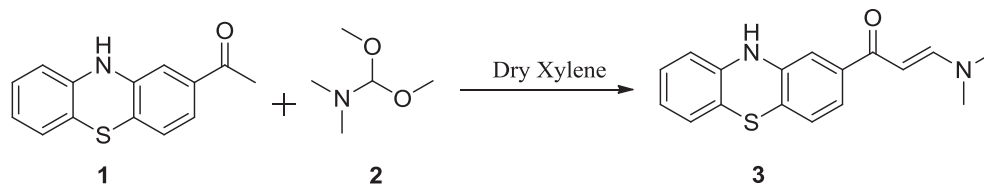
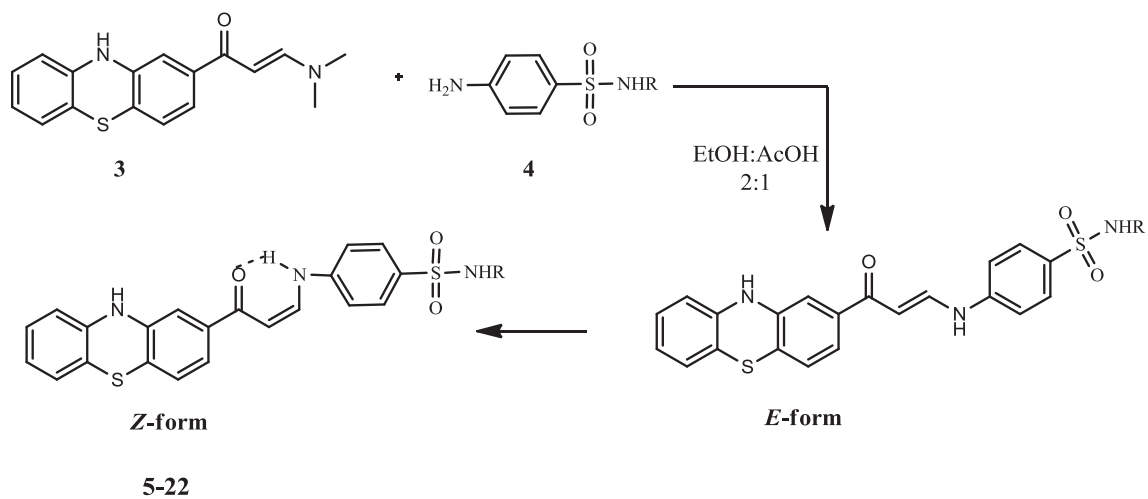


Fig. 2. Binding mode of both lead compound (B) and one of the newly designed series, compound **18**.



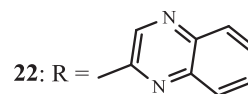
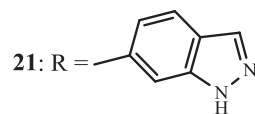
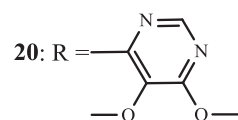
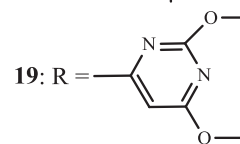
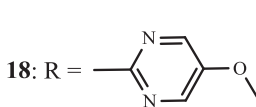
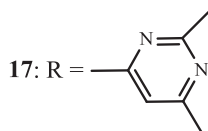
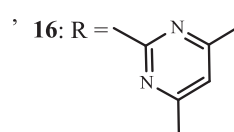
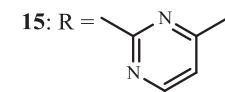
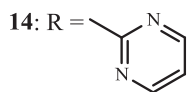
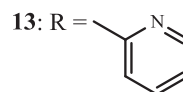
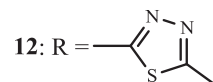
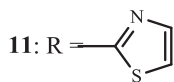
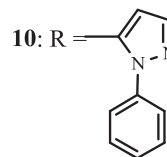
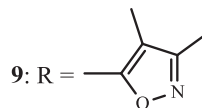
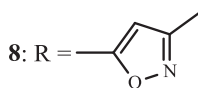
Scheme 1. Synthetic pathway for compound 3.



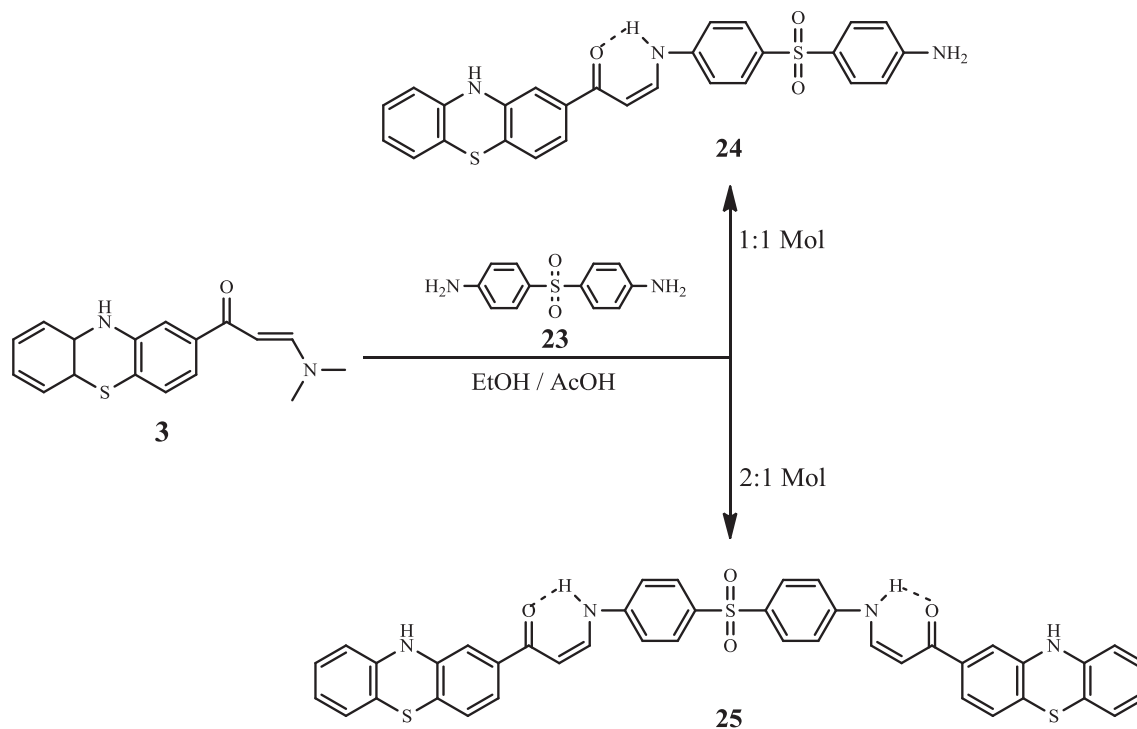
5: R = H,

6: R = COCH₃

7: R =



Scheme 2. Synthetic pathway for compounds 5–22.



Scheme 3. Synthetic pathways for compounds **24** and **25**.

Table 1
Anticancer and aromatase inhibition activity of the newly synthesized compounds **3**, **5–22**, **24** and **25**.

Compound No.	IC ₅₀ against T47D (μM)	% inhibition of aromatase enzyme	IC ₅₀ of aromatase enzyme (μM)
3	135.8	ND	ND
5	67.6	28.9	ND
6	71.8	40.52	ND
7	23.7	72.22	9.67
8	78.4	ND	ND
9	79.5	ND	ND
10	68.1	ND	ND
11	8.1	68.32	5.67
12	71.4	ND	ND
13	8.8	68.86	6.7
14	61.3	30.82	ND
15	73.6	ND	ND
16	50.7	43.62	ND
17	56.5	35.88	ND
18	83.2	ND	ND
19	58.1	44.94	ND
20	82.2	ND	ND
21	91.1	ND	ND
22	21.4	65.10	8.9
24	54.9	31.92	ND
25	46.4	ND	ND
Doxorubicin	9.8	–	–
Letrozole	–	58	29.5

*ND: Not Done.

twice that of letrozole (Fig. 3). To trace compound **11** apoptotic mechanism whether it is through the induction of the intrinsic or the extrinsic pathway or both, its effect on caspases 8 and 9 was also evaluated. It has been found that compound **11** increased the levels of caspases 8 and 9 by 34, and 8.9 folds, respectively compared to the control cells, which indicates activation of both intrinsic and extrinsic pathways. (Table 2, Fig. 3).

2.2.3.2. Effects on Bcl-2 family proteins. The B-cell lymphoma

protein 2 (Bcl-2) family plays a key role in tumor progression or inhibition of intrinsic apoptotic pathway triggered by mitochondrial dysfunction, with Bcl-2 itself and Bcl-X_L (also known as Bcl2L1) as anti-apoptotic and Bcl-2-associated X protein (BAX) as pro-apoptotic proteins [19]. The effect of compound **11** on the expression levels of Bcl2, Bcl-X_L and BAX was determined after treatment of T47D cells with the IC₅₀ of compound **11**, and the results were illustrated in Table 3.

Compound **11** caused upregulation in the level of the

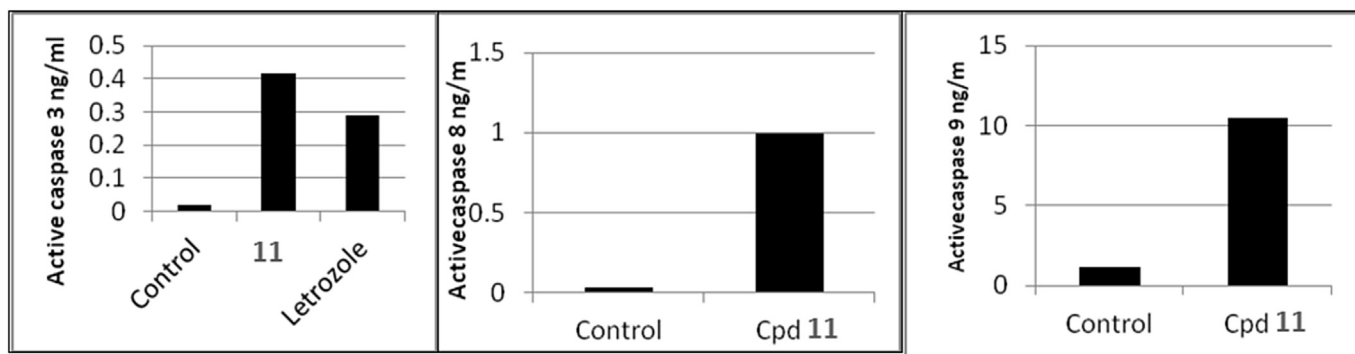


Fig. 3. The effect of compound **11** on the active caspases 3 versus letrozole as a reference compound, and on caspases 8 and 9 in T47D cells.

Table 2

Effect of compound **11** on the active caspases 3, 8 and 9 in T47D cells.

Sample code	Caspase 3 ng/mL	Caspase 8 ng/mL	Caspase 9 ng/mL
11	0.418042	0.995	10.5136
Control	0.0208912	0.029	1.18753

Table 3

Effect of compound **11** on the expression of the gene of some apoptosis key markers.

Sample code	BAX IU/ml	BCL2 IU/ml	BCL-X _L IU/ml
11	137,308	298	Below the detectable level
Control	24.6	568,019	754,565

proapoptotic protein; BAX by approximately 55,000 folds while it markedly downregulated the levels of the antiapoptotic proteins Bcl2 to 5.24×10^{-4} and Bcl-X_L to an undetectable level, compared to the control. From literature survey, there is strong evidence that the ratio of pro-apoptotic BAX versus anti-apoptotic Bcl-2 proteins indicates the susceptibility of cancer cells to undergo apoptosis more accurately [20]. According to our results, compound **11** increased the BAX/Bcl2 ratio by approximately 10^8 folds as compared to the control. These findings proved the proapoptotic effect of compound **11**.

2.2.3.3. Cell cycle analysis [21]. To gain further insight into the mode of action of compound **11**, the most potent one, we examined its effect at IC₅₀ (8.1 μM) on the cell cycle by flow cytometry in T47D cells. The results obtained following cell cycle analysis of both untreated control cells and cells treated with compound **11** (Fig. 4) interestingly showed a concentration-dependent change in the cell cycle pattern. These results clearly demonstrate that a significant increase in the percentage of cell population at the G2/M phase (56.3%) was produced by treatment of the cells with compound **11** (Fig. 4A) when compared to untreated control (15.81%) (Fig. 4 B). This implies that the cell cycle of the treated cells was arrested at G2/M phase. Also, the cell population in G1 and S phases were markedly decreased after treatment (7.4% and 13.1% versus 64.92% and 17.14%, respectively). From these results, it was disclosed that, cell cycle arrest in T47D cells in the G2/M phase contributes to compound **11** cytotoxicity.

2.2.3.4. Cell viability test. The cytotoxic effect of compound **11**, being the most potent synthesized compound, was tested on the normal breast cells 184A1 [22] using SRB assay. Compound **11** showed mild cytotoxic effect with an IC₅₀ of 391.3 μM. This result indicates the selectivity of compound **11** towards breast cancer cells and its relative safety for normal breast cells (Fig. 5).

2.3. Molecular modeling studies

2.3.1. Molecular docking

In general, hydrophobicity and H-bonding interactions are the important features for fitting in the aromatase active site. The 3D ligand-protein interaction of the co-crystallized natural substrate androstenedione (ASD) (Fig. 6) displayed hydrogen bonding of the CO group at position 17 with the amino acid Met 374, with an interaction energy = $-44.54 \text{ kcal mol}^{-1}$ [23].

In order to investigate the binding mode of phenothiazines **5–22**, **24** and **25** to the aromatase enzyme, redocking of the co-crystallized ligand was performed in order to validate the docking procedure. The redocked ligand was found to completely superimpose on the co-crystallized one (Fig. 6B). The target compounds were fit into the aromatase active site with low C-DOCKER interaction energy. Compound **11** forms hydrogen bonds with Met 374 and Leu 372 using the sulfonamide oxygen and nitrogen, respectively with an interaction energy = $-49.18 \text{ kcal mol}^{-1}$ (Fig. 7). This further gives insight to the significant role of sulfonamide group to the anticancer activity as early observed when comparing compound **3** (IC₅₀ = 135.8 μM) which is devoid of a sulfonamide group.

2.3.2. ADMET studies

Computer aided ADMET study was done by using the software Accord for Excel (Accelrys Discovery studio 2.5 software). These studies are solely based on the chemical structure of the molecule. All the parameters calculated are tabulated (Table 4). The ADMET-Plot is a 2D plot using calculated PSA_{2D} and A logp98 properties. Blood Brain Barrier (BBB) and Human Intestinal Absorption (HIA) plots (Fig. 7) were drawn using all the compounds. In BBB plot all the 20 compounds fall outside the 99% ellipse (undefined). Hence, these compounds may not be able to penetrate the blood brain barrier, the chances of CNS side effects are low or absent. In HIA plot 11 compounds fall outside the 99% confidence ellipse (low absorption), whereas the remaining compounds fall inside the 99% ellipse. Hence compounds **5** and **6** have unsubstituted sulfonamide and *N*-sulfonyl acetamide are expected to possess good human intestinal absorption. Compounds **8**, **11**, **12**, **13**, **14**, **15** and **17** showed moderate absorption as they have high molecular weights. ADME Aqueous solubility logarithmic level of most of the compounds was found to be 2 or 1, which indicates very little aqueous solubility. The hepatotoxicity score predicts the hepatotoxic nature of the chemical compounds. The ADME.HEPATOTOX.PROB values of most of the compounds lie in the range of 0.715–0.966. Hence the compounds are likely to possess hepatotoxicity, further studies are necessary to determine the hepatotoxic dose levels. The CYP2D6 score predicts the inhibitory and non-inhibitory character of the given query chemical structure on Cytochrome P450 2D6 enzyme. All the

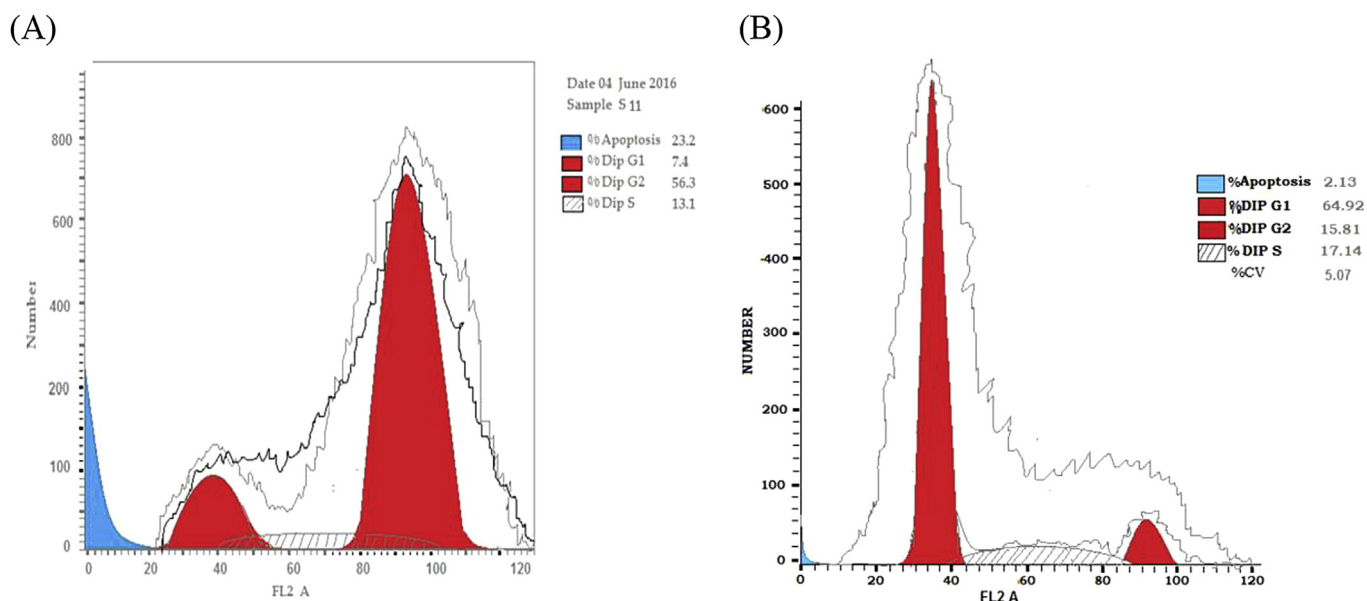


Fig. 4. (A) Effect of compound **11** on the phases of the cell cycle in T47D cells. (B) Cell cycle phases in untreated cells.

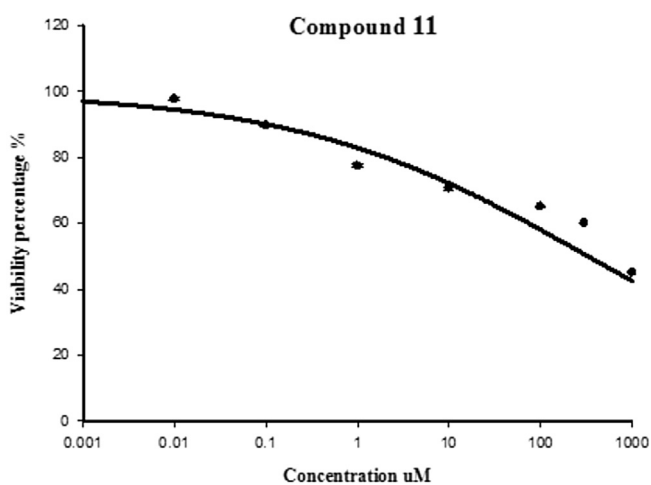


Fig. 5. The effect of compound **11** on the viability percentage of 184A1 normal breast cells.

compounds are predicted as non-inhibitors of CYP2D6, so the side effects (i.e. liver dysfunction) are not expected upon administration of these compounds. The plasma protein-binding model predicts whether a compound is likely to be highly bound to carrier proteins

in the blood. There is a high probability that these compounds can reach the desired targets as all of the compounds showed more than 95% plasma protein binding. PSA is a key property that has been linked to drug bioavailability. Thus, passively absorbed molecules with PSA >140 are thought to have low bioavailability. All the synthesized compounds have PSA ranging from 104.062 to 139.96 they theoretically should present good passive oral absorption (Fig. 8).

2.4. Structure activity relationship (SAR)

Replacement of the coumarin ring in lead compounds (**A**) and (**B**) with phenothiazine ring was found to greatly enhance the cytotoxic activity [13]. The thiazolyl derivative **11** and the pyridinyl derivative **13** revealed the most potent cytotoxic activity against human breast cancer cell line (T47D) (IC_{50} 8.1 and 8.8 μ M), this gives an indication that the introduction of a substituted sulfonamide group is more favorable than the unsubstituted and could enhance the activity. The most potent cytotoxic compounds were screened for their aromatase inhibitory profile, compounds **11** and **13** showed the highest percentage inhibition and the lowest IC_{50} towards the aromatase enzyme (IC_{50} 5.67 and 6.70 μ M). Followed by the quinoxaliny derivative **22**, that showed moderate cytotoxicity (IC_{50} 21.4 μ M), but high percentage inhibition and low IC_{50} towards the aromatase enzyme (IC_{50} 8.90 μ M). The mono and

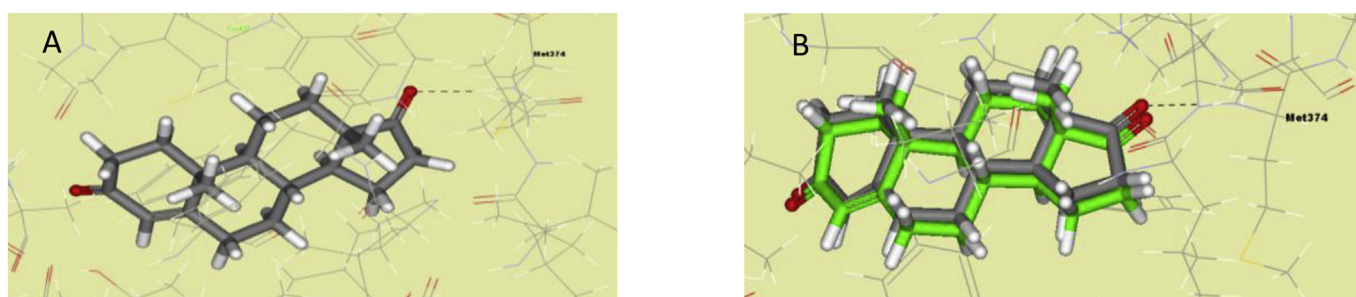


Fig. 6. (A) 3D ligand-protein interaction of the co-crystallized ASD with aromatase enzyme (PDB:3EQM). (B) Redocking of the co-crystallized ASD yielded RMSD of 0.448 Å.

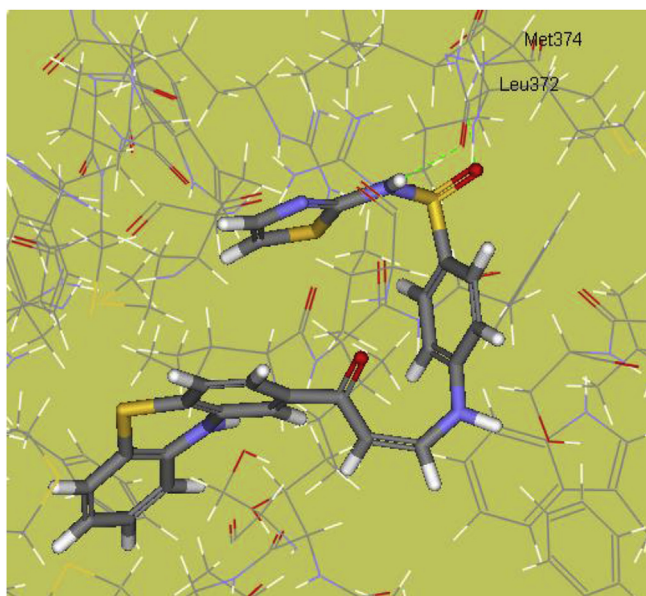


Fig. 7. 3D ligand-protein interaction of compound **11** with aromatase enzyme (PDB:3EQM).

disubstituted derivatives **24** and **25** were found to possess moderate to poor cytotoxic activity and low percentage inhibition towards the enzyme tested. Accordingly, the thiazolyl derivative **11** was investigated for its apoptotic effect and showed a marked increase in Bax level, and down-regulation in Bcl2. Furthermore, the effect on caspases 3, 8 and 9 was evaluated and was found to increase their levels by 20, 34, and 8.9 folds, respectively, which indicates the activation of both intrinsic and extrinsic pathways. Cell cycle analysis indicated that compound **11** arrested the cell cycle at G2/M phase. Finally, according to computer aided ADMET studies,

compounds **11** and **13** was found to show moderate absorption in human intestine.

3. Conclusion

Twenty novel phenothiazine derivatives bearing sulfonamide moiety were designed and synthesized as aromatase inhibitors. All the newly prepared compounds were evaluated for their *in vitro* anticancer activity against T47D cell line, where they showed anticancer activities with IC₅₀ values ranging from 8.1 to 91.1 μM. In order to investigate their aromatase inhibitory effect, eleven compounds were tested against the target enzyme, where compound **7** produced the greatest inhibitory effect (72.2%) with IC₅₀ = 9.67 μM, and compound **11** bearing unsubstituted thiazole ring produced a good inhibitory effect (68.32%) and the lowest IC₅₀ value (5.67 μM). Further investigations were performed to prove the proapoptotic effect of our target compounds. Compound **11** showed a marked increase in BAX level and downregulation in Bcl2 and Bcl-X_L to undetectable levels, in comparison to the control. To figure out the apoptotic mechanism of compound **11**, its effect on caspases 3, 8 and 9 was evaluated and found to increase their levels by activation of both intrinsic and extrinsic pathways of apoptosis. Finally, molecular modeling studies were carried out. First, molecular docking which showed that phenothiazine series binds to the target enzyme in the same pattern as androstenedione “the natural ligand” and that the phenothiazine ring fits into the large hydrophobic pocket in the binding site. Second, computer aided ADMET study was performed, compounds **5** and **6** having unsubstituted sulfonamide and *N*-sulfonyl acetamide, respectively were expected to possess good human intestinal absorption.

4. Experimental

4.1. Chemistry

Melting points (uncorrected) were determined in an open

Table 4
Computer aided ADMET screening results of the prepared compounds.

CPD ID	BBB_ Lev ^a	Absorp_ Lev ^b	AQ SOI LEV ^c	Hepatox ^d	Hepatox Prob	CYP 2D6 ^e	PPB_ Lev ^f	A log P98	Unk_Alog P98	ADEM_PSA_2D ^g
5	4	0	2	1	0.953	0	2	3.586	0	104.062
6	4	0	2	1	0.887	0	2	3.576	0	107.633
7	4	2	2	1	0.947	0	2	3.421	0	139.96
8	4	1	2	1	0.92	0	2	4.23	0	114.148
9	4	2	1	1	0.907	0	2	4.716	0	114.148
10	4	2	1	1	0.947	0	2	5.72	0	106.942
11	4	1	1	1	0.94	0	2	4.559	0	101.594
12	4	1	1	1	0.92	0	2	4.57	0	112.855
13	4	1	2	1	0.953	0	2	4.757	0	101.594
14	4	1	2	1	0.894	0	2	4.111	0	112.855
15	4	1	2	1	0.913	0	2	4.394	0	112.855
16	4	2	2	1	0.715	0	2	4.676	0	112.855
17	4	1	2	1	0.92	0	2	4.368	0	112.855
18	4	2	2	1	0.887	0	2	4.095	0	121.785
19	4	2	1	1	0.887	0	2	5.157	0	130.715
20	4	2	1	1	0.821	0	2	4.636	0	130.715
21	4	2	1	1	0.953	0	2	5.013	0	116.649
22	4	2	1	1	0.94	0	2	5.372	0	112.855
24	4	2	1	1	0.96	0	2	5.237	0	104.062
25	4	3	1	1	0.966	0	2	9.036	0	120.444

^a BBB_Level; 4 = undefined, 2 = medium penetration, 1 = high penetration.

^b Absop_Level; 3 = very low absorption, 2 = low absorption, 1 = moderate, 0 = good absorption.

^c AQ SOI_LEV; 2 = low solubility, 1 = very low but soluble, 0 = extremely low.

^d Hepatotox_Level; 1 = toxic, 0 = non toxic.

^e Cyp 2D6; 1 = likely to inhibit, 0 = non inhibitor.

^f PPB (Plasma protein binding); 2 = more than 95%, 1 = more than 90%, 0 = less than 90%.

^g PSA (polar surface area); cpds must have log p value not greater than 5.0 to attain a reasonable probability of being well absorbed.

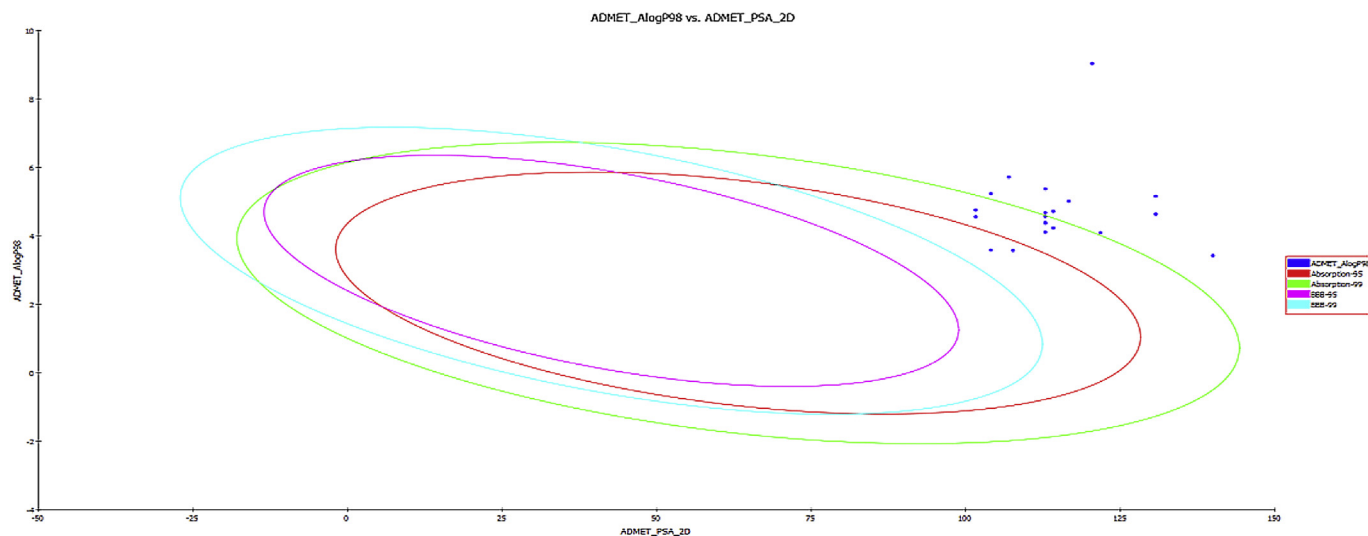


Fig. 8. Human intestinal absorption (HIA) and Blood Brain Barrier plot for the newly synthesized compounds.

capillary on a Gallen Kamp melting point apparatus (Sanyo Gallen Kamp, UK). Precoated silica gel plates (*Kieselgel* 0.25 mm, 60 F254, Merck, Germany) were used for thin layer chromatography. A developing solvent system of chloroform/methanol (8:2) was used and the spots were detected by ultraviolet light. IR spectra (KBr discs) were recorded using an FT-IR spectrophotometer (Perkin Elmer, USA). ^1H NMR spectra were scanned on an NMR spectrophotometer (Bruker AXS Inc., Switzerland), operating at 500 MHz for ^1H and 125.76 MHz for ^{13}C . Chemical shifts are expressed in (ppm) -values relative to TMS as an internal standard, using $\text{DMSO}-d_6$ as a solvent. Elemental analyses were done on a model 2400 CHNSO analyzer (Perkin Elmer, USA). All the values were within $\pm 0.4\%$ of the theoretical values. All reagents used were of AR grade. The starting material 1-(10H-phenothiazin-2-yl) ethanone **1** was purchased from sigma (USA) and was directly used for the preparation of the target compounds.

4.1.1. (Z)-3-(dimethylamino)-1-(10H-phenothiazin-2-yl) prop-2-en-1-one (**3**)

To a solution of **1** (2.41 g, 0.01 mol) in dry xylene (20 mL) dimethylformamide-dimethylacetal (DMF-DMA) **2** (1.91 g, 0.015 mol) was added and refluxed for 24 h. The obtained solid was collected by filtration and crystallized from ethanol to give compound **3**.

Yield, 81%; m.p. 247.0 °C. IR: 3257 (NH), 3051 (arom.), 2970, 2846 (aliph.), 1637 (CO). ^1H NMR: 3.1 (s, 6H, $\text{N}(\text{CH}_3)_2$), 5.7, 7.7 (2d, 2H, $\text{CH}=\text{CH}$, $J = 12.5$ Hz), 6.9–7.3 (m, 7H, Ar-H), 8.6 (s, 1H, NH). ^{13}C NMR: 44.9 (2), 91.0, 113.1, 114.9 (2), 116.1, 120.4, 122.3, 126.1, 126.7, 128.2, 140.0, 142.1, 142.4, 154.6, 185.1. MS m/z (%): 296 (M^+) (10.37), 227 (100). Anal. Calcd. for $\text{C}_{17}\text{H}_{16}\text{N}_2\text{OS}$ (296.39): C, 68.89; H, 5.44; N, 9.45. Found: C, 68.56; H, 5.11; N, 9.13.

4.1.2. General procedure for the synthesis of benzenesulfonamide derivatives (**5**–**22**)

A mixture of **3** (2.96 g, 0.01 mol) and sulfa drugs **4** (0.012 mol) in absolute ethanol (10 mL) and glacial acetic acid (3 mL) was refluxed for 18 h. The solid product formed was collected by filtration and crystallized from ethanol to give **5**–**22**.

4.1.2.1. (Z)-4-(3-Oxo-3-(10H-phenothiazin-2-yl) prop-1-enylamino) benzenesulfonamide (**5**). Yield, 61%; m.p. 299.4 °C. IR: 3344, 3248 (NH_2 , NH), 3085 (arom.), 2943, 2863 (aliph.), 1660 (2CO), 1334, 1186

(SO_2). ^1H NMR: 6.0, 7.9 (2d, 2H, $\text{CH}=\text{CH}$, $J = 10$ Hz), 6.6–7.8 (m, 11H, Ar-H), 8.7 (s, 1H, SO_2NH_2), 10.3 (s, 1H, NH, phenothiazine), 11.9 (s, 1H, NH). ^{13}C NMR: 94.9, 112.7, 113.0 (2), 115.0, 115.5, 115.9, 116.4, 121.4, 122.5, 126.5, 127.9, 128.1, 128.3 (2), 128.4, 137.5, 141.8 (2), 143.3, 189.4. MS m/z (%): 423 (M^+) (8.28), 198 (100). Anal. Calcd. for $\text{C}_{21}\text{H}_{17}\text{N}_3\text{O}_3\text{S}_2$ (423.51): C, 59.56; H, 4.05; N, 9.92. Found: C, 59.84; H, 4.33; N, 10.06.

4.1.2.2. (Z)-N-4-(3-Oxo-3-(10H-phenothiazin-2-yl) prop-1-enylamino) phenylsulfonylacetamide (**6**). Yield, 84%; m.p. 278.8 °C. IR: 3305, 3248 (NH), 3055 (arom.), 2931, 2836 (aliph.), 1737, 1635 (2CO), 1363, 1190 (SO_2). ^1H NMR: 1.9 (s, 3H, COCH_3), 6.1, 7.5 (2d, 2H, $\text{CH}=\text{CH}$, $J = 10.5$ Hz), 6.7–7.4 (m, 11H, Ar-H), 8.7 (s, 2H, SO_2NH), 10.4 (s, 1H, NH phenothiazine), 10.5 (s, 1H, NH). ^{13}C NMR: 23.7, 95.6, 112.7, 113.0 (2), 115.0, 115.3, 115.9, 116.3, 121.5, 122.1, 126.5, 126.6, 126.7, 128.3 (2), 128.4, 138.1, 141.7 (2), 142.5, 169.2, 189.5. MS m/z (%): 465 (M^+) (43.14), 267 (100). Anal. Calcd. for $\text{C}_{23}\text{H}_{19}\text{N}_3\text{O}_4\text{S}_2$ (465.54): C, 59.34; H, 4.11; N, 9.03. Found: C, 59.03; H, 4.00; N, 8.95.

4.1.2.3. (Z)-N-carbamimidoyl-4-(3-oxo-3-(10H-phenothiazin-2-yl) prop-1-enylamino) benzenesulfonamide (**7**). Yield, 77%; m.p. 285.4 °C. IR: 3429, 3354, 3196 (NH_2 , NH), 3088 (arom.), 2954, 2854 (aliph.), 1635 (CO), 1589 (CN), 1319, 1132 (SO_2). ^1H NMR: 6.1, 7.9 (2d, 2H, $\text{CH}=\text{CH}$, $J = 10.5$ Hz), 6.9–7.8 (m, 12H, Ar-H), 8.1 (s, 1H, SO_2NH), 8.7 (s, 2H, NH_2), 10.3 (s, 2H, NH, phenothiazine + NH imino), 11.9 (s, 1H, NH). ^{13}C NMR: 94.7, 112.7 (2), 113.0, 115.0 (2), 115.9, 116.3, 121.4, 122.2, 126.5, 127.7, 127.9 (2), 128.3, 138.2, 141.8, 142.5, 143.8, 145.3, 158.5, 189.3. MS m/z (%): 465 (M^+) (0.98), 388 (100). Anal. Calcd. for $\text{C}_{22}\text{H}_{19}\text{N}_5\text{O}_3\text{S}_2$ (465.55): C, 56.76; H, 4.11; N, 15.04. Found: C, 56.45; H, 4.00; N, 14.89.

4.1.2.4. (Z)-N-(3-methylisoxazol-5-yl)-4-(3-oxo-3-(10H-phenothiazin-2-yl) prop-1-enylamino) benzenesulfonamide (**8**). Yield, 85%; m.p. 270.5 °C. IR: 3388, 3298, 3161 (NH), 3045 (arom.), 2912, 2871 (aliph.), 1635 (CO), 1591 (CN), 1381, 1161 (SO_2). ^1H NMR: 2.3 (s, 3H, CH_3), 6.1, 7.4 (2d, 2H, $\text{CH}=\text{CH}$, $J = 10.1$ Hz), 6.2 (s, 1H, CH isoxazole), 6.7–7.3 (m, 11H, Ar-H), 8.7 (s, 1H, SO_2NH), 10.4 (s, 1H, NH phenothiazine), 11.9 (s, 1H, NH). ^{13}C NMR: 12.5, 95.5, 100.4, 112.7, 115.0 (2), 115.7 (2), 115.9, 116.7, 121.5, 126.5, 126.7, 128.3, 129.1, 129.3, 132.1 (2), 138.8, 141.4 (2), 144.7, 158.0, 158.1, 189.5. MS m/z (%): 504 (M^+) (18.53), 333 (100). Anal. Calcd. for $\text{C}_{25}\text{H}_{20}\text{N}_4\text{O}_4\text{S}_2$ (504.58): C, 59.51;

H, 4.00; N, 11.10. Found: C, 59.22; H, 3.87; N, 10.84.

4.1.2.5. (*Z*)-*N*-(3,4-Dimethylisoxazol-5-yl)-4-(3-oxo-3-(10*H*-phenothiazine-2-yl) prop-1-enylamino) benzenesulfonamide (**9**). Yield, 69%; m.p. 277.5 °C. IR: 3309, 3272 (NH), 3016 (arom.), 2823, 2765 (aliph.), 1634 (CO), 1583 (CN), 1375, 1186 (SO₂). ¹H NMR: 2.1, 2.2 (2s, 6H, 2CH₃), 6.1, 7.5 (2d, 2H, CH=CH, *J* = 10 Hz), 6.7–7.4 (m, 11H, Ar-H), 8.7 (s, 1H, SO₂NH), 10.4 (s, 1H, NH, phenothiazine), 11.9 (s, 1H, NH). ¹³C NMR: 6.3, 10.7, 95.6, 100.5, 112.7, 113.0 (2), 115.0, 115.7, 115.9, 116.7, 121.5, 122.1, 126.5, 126.7, 128.3, 129.0, 129.2 (2), 138.8, 141.7 (2), 143.2, 156.1, 161.8, 187.1. MS *m/z* (%): 518 (M⁺) (9.43), 266 (100). Anal. Calcd. for C₂₆H₂₂N₄O₄S₂ (518.61): C, 60.21; H, 4.28; N, 10.80. Found: C, 62.54; H, 4.58; N, 11.15.

4.1.2.6. (*Z*)-4-(3-Oxo-3-(10*H*-phenothiazine-2-yl) prop-1-enylamino)-*N*-(1-phenyl-1*H*-pyrazol-5-yl)-benzenesulfonamide (**10**). Yield, 88%; m.p. 258.9 °C. IR: 3409, 3374 (NH), 3062 (arom.), 2816, 2742 (aliph.), 1635 (CO), 1589 (CN), 1390, 1157 (SO₂). ¹H NMR: 5.9 (d, 2H, 2CH pyrazole, *J* = 10 Hz), 6.1, 7.5 (2d, 2H, CH=CH, *J* = 10.5 Hz), 6.8–7.4 (m, 18H, Ar-H), 8.9 (s, 1H, SO₂NH), 10.4 (s, 1H, NH, phenothiazine), 11.9 (s, 1H, NH). ¹³C NMR: 95.5, 104.3, 112.8, 113.0 (2), 115.0, 115.6 (2), 116.6, 121.5, 122.1 (2), 124.7, 126.5, 126.6, 126.7, 127.9, 128.3 (2), 129.1, 132.2 (2), 135.0, 138.1, 140.0, 142.5 (2), 143.3, 145.5, 187.1. MS *m/z* (%): 565 (M⁺) (0.76), 488 (100). Anal. Calcd. for C₃₀H₂₃N₅O₃S₂ (565.67): C, 63.70; H, 4.10; N, 12.38. Found: C, 63.43; H, 3.79; N, 12.02.

4.1.2.7. (*Z*)-4-(3-Oxo-3-(10*H*-phenothiazine-2-yl) prop-1-enylamino)-*N*-(thiazol-2-yl) benzenesulfonamide (**11**). Yield, 90%; m.p. 282.4 °C. IR: 3392, 3187 (NH), 3066 (arom.), 2946, 2852 (aliph.), 1637 (CO), 1587 (CN), 1361, 1139 (SO₂). ¹H NMR: 6.0, 7.3 (2d, 2H, CH=CH, *J* = 10.1 Hz), 6.7–7.2 (m, 13H, Ar-H), 8.7 (s, 1H, SO₂NH), 10.3 (s, 1H, NH phenothiazine), 11.9 (s, 1H, NH). ¹³C NMR: 95.0, 108.6, 112.7, 112.9 (2), 113.0, 115.5 (2), 116.4, 121.4, 122.3, 126.5, 126.7, 128.1, 128.2, 128.3 (2), 135.6, 141.8, 142.5 (2), 143.6, 169.9, 187.0. MS *m/z* (%): 506 (M⁺) (2.54), 351 (100). Anal. Calcd. for C₂₄H₁₈N₄O₃S₃ (506.62): C, 56.90; H, 3.58; N, 11.06. Found: C, 56.61; H, 3.26; N, 10.78.

4.1.2.8. (*Z*)-*N*-(5-Methyl-1,3,4-thiadiazol-2-yl)-4-(3-oxo-3-(10*H*-phenothiazine-2-yl) prop-1-enylamino) benzenesulfonamide (**12**). Yield, 77%; m.p. 274.0 °C. IR: 3304, 3198 (NH), 3034 (arom.), 2883, 2814, (aliph.), 1633 (CO), 1589 (CN), 1363, 1149 (SO₂). ¹H NMR: 2.4 (s, 3H, CH₃), 6.1, 7.4 (2d, 2H, CH=CH, *J* = 10.5 Hz), 6.6–7.3 (m, 11H, Ar-H), 8.7 (s, 1H, SO₂NH), 10.3 (s, 1H, NH phenothiazine), 11.9 (s, 1H, NH). ¹³C NMR: 16.5, 95.2, 112.7, 113.0 (2), 115.0, 115.6 (2), 116.6, 121.4, 122.0, 126.5, 126.7, 128.0, 128.2, 128.3 (2), 141.8, 142.5 (2), 143.4, 144.9, 168.2, 187.0. MS *m/z* (%): 521 (M⁺) (33.62), 323 (100). Anal. Calcd. for C₂₄H₁₉N₅O₃S₃ (521.63): C, 55.26; H, 3.67; N, 13.43. Found: C, 54.91; H, 3.32; N, 13.11.

4.1.2.9. (*Z*)-4-(3-Oxo-3-(10*H*-phenothiazine-2-yl) prop-1-enylamino)-*N*-(pyridin-2-yl) benzenesulfonamide (**13**). Yield, 88%; m.p. 263.4 °C. IR: 3450, 3358 (NH), 3100 (arom.), 2945, 2872 (aliph.), 1633 (CO), 1591 (CN), 1386, 1134 (SO₂). ¹H NMR: 6.1, 7.4 (2d, 2H, CH=CH, *J* = 10 Hz), 6.6–7.3 (m, 15H, Ar-H), 8.5 (s, 1H, SO₂NH), 10.3 (s, 1H, NH phenothiazine), 11.9 (s, 1H, NH). ¹³C NMR: 95.1, 112.7, 112.9, 113.0 (2), 114.0, 115.4, 115.7, 115.9, 116.4, 121.4, 122.3, 126.5, 126.7, 128.3, 128.9, 129.2 (2), 138.1, 141.7, 143.5 (2), 144.8, 144.9, 153.2, 187.0. MS *m/z* (%): 500 (M⁺) (0.99), 267 (100). Anal. Calcd. for C₂₆H₂₀N₄O₃S₂ (500.59): C, 62.38; H, 4.03; N, 11.19. Found: C, 62.08; H, 3.83; N, 11.01.

4.1.2.10. (*Z*)-4-(3-Oxo-3-(10*H*-phenothiazine-2-yl) prop-1-enylamino)-*N*-(pyrimidin-2-yl) benzenesulfonamide (**14**). Yield,

69%; m.p. 309.9 °C. IR: 3358, 3110 (NH), 3037 (arom.), 2941, 2870 (aliph.), 1633 (CO), 1585 (CN), 1373, 1195 (SO₂). ¹H NMR: 6.0, 7.6 (2d, 2H, CH=CH, *J* = 10 Hz), 6.7–7.5 (m, 14H, Ar-H), 8.4 (s, 1H, SO₂NH), 10.4 (s, 1H, NH phenothiazine), 11.6 (s, 1H, NH). ¹³C NMR: 95.4, 112.6, 112.7 (2), 113.0, 115.0, 115.9 (2), 116.2, 121.5, 122.0, 125.4, 126.5, 126.7, 128.3, 130.0 (2), 141.7, 142.5 (2), 144.3, 157.4 (2), 158.8, 187.1. MS *m/z* (%): 501 (M⁺) (7.46), 342 (100). Anal. Calcd. for C₂₅H₁₉N₅O₃S₂ (501.58): C, 59.86; H, 3.82; N, 13.96. Found: C, 59.57; H, 3.65; N, 13.60.

4.1.2.11. (*Z*)-*N*-(4-Methylpyrimidin-2-yl)-4-(3-oxo-3-(10*H*-phenothiazine-2-yl) prop-1-enylamino) benzenesulfonamide (**15**). Yield, 90%; m.p. 302.0 °C. IR: 3371, 3162 (NH), 3032 (arom.), 2960, 2870 (aliph.), 1635 (CO), 1589 (CN), 1373, 1157 (SO₂). ¹H NMR: 2.3 (s, 3H, CH₃), 6.0, 7.5 (2d, 2H, CH=CH, *J* = 10.1 Hz), 6.6–7.4 (m, 13H, Ar-H), 8.3 (s, 1H, SO₂NH), 10.4 (s, 1H, NH phenothiazine), 11.9 (s, 1H, NH). ¹³C NMR: 23.7, 95.3, 112.4, 112.7, 113.0 (2), 115.0, 115.2, 115.8, 115.9, 121.5, 122.0, 125.4, 126.5, 126.7, 128.3, 130.2 (2), 141.8, 142.5 (2), 143.4, 153.4, 168.4, 168.6, 187.0. MS *m/z* (%): 515 (M⁺) (6.93), 198 (100). Anal. Calcd. for C₂₆H₂₁N₅O₃S₂ (515.61): C, 60.57; H, 4.11; N, 13.58. Found: C, 60.24; H, 4.06; N, 13.27.

4.1.2.12. (*Z*)-*N*-(4,6-Dimethylpyrimidin-2-yl)-4-(3-oxo-3-(10*H*-phenothiazine-2-yl) prop-1-enylamino) benzenesulfonamide (**16**). Yield, 91%; m.p. 271.8 °C. IR: 3360, 3116 (NH), 3100 (arom.), 2961, 2836 (aliph.), 1633 (CO), 1587 (CN), 1371, 1192 (SO₂). ¹H NMR: 2.2 (s, 6H, 2CH₃), 6.0 (s, 1H, CH pyrimidine), 6.4, 7.5 (2d, 2H, CH=CH, *J* = 10 Hz), 6.6–7.4 (m, 12H, Ar-H), 8.5 (s, 1H, SO₂NH), 10.3 (s, 1H, NH phenothiazine), 11.9 (s, 1H, NH). ¹³C NMR: 23.5 (2), 95.2, 112.7, 113.0, 113.9 (2), 114.9, 115.0, 115.8, 115.9, 121.5, 126.5, 126.7, 128.3, 130.5, 130.7, 133.5 (2), 141.7, 143.4 (2), 145.0, 167.8 (2), 172.5, 187.0. MS *m/z* (%): 529 (M⁺) (17.62), 262 (100). Anal. Calcd. for C₂₇H₂₃N₅O₃S₂ (529.63): C, 61.23; H, 4.38; N, 13.22. Found: C, 61.02; H, 4.10; N, 13.16.

4.1.2.13. (*Z*)-*N*-(2,6-Dimethylpyrimidin-2-yl)-4-(3-oxo-3-(10*H*-phenothiazine-2-yl) prop-1-enylamino) benzenesulfonamide (**17**). Yield, 86%; m.p. 261.3 °C. IR: 3372, 3210 (NH), 3100 (arom.), 2971, 2836 (aliph.), 1637 (CO), 1589 (CN), 1373, 1199 (SO₂). ¹H NMR: 2.2, 2.3 (2s, 6H, 2CH₃), 6.0, 7.5 (2d, 2H, CH=CH, *J* = 10 Hz), 6.6–7.4 (m, 12H, Ar-H), 8.7 (s, 1H, SO₂NH), 10.3 (s, 1H, NH phenothiazine), 11.9 (s, 1H, NH). ¹³C NMR: 23.2, 23.9, 95.8, 105.0, 112.7, 113.0 (2), 115.0, 115.3, 115.9, 116.2, 121.9, 126.5, 126.7, 128.3, 128.8, 128.9, 129.1 (2), 141.8, 142.5 (2), 143.5, 154.2, 163.8, 164.6, 187.0. MS *m/z* (%): 529 (M⁺) (34.36), 222 (100). Anal. Calcd. for C₂₇H₂₃N₅O₃S₂ (529.63): C, 61.23; H, 4.38; N, 13.22. Found: C, 61.52; H, 4.76; N, 13.41.

4.1.2.14. (*Z*)-*N*-(5-Methoxypyrimidin-2-yl)-4-(3-oxo-3-(10*H*-phenothiazine-2-yl) prop-1-enyl-amino) benzenesulfonamide (**18**). Yield, 84%; m.p. 281.5 °C. IR: 3363, 3294 (NH), 3100 (arom.), 2929, 2839 (aliph.), 1635 (CO), 1591 (CN), 1338, 1153 (SO₂). ¹H NMR: 3.7 (s, 3H, OCH₃), 6.0, 7.5 (2d, 2H, CH=CH, *J* = 10.5 Hz), 6.5–7.4 (m, 13H, Ar-H), 8.7 (s, 1H, SO₂NH), 10.4 (s, 1H, NH phenothiazine), 11.9 (s, 1H, NH). ¹³C NMR: 56.7, 95.3, 112.6, 112.7 (2), 113.0, 115.0, 115.8, 116.2, 121.4, 125.7, 126.5, 128.3, 129.8, 130.1, 133.3 (2), 141.7 (2), 142.5, 143.4 (2), 144.2, 144.9, 162.0, 187.0. MS *m/z* (%): 531 (M⁺) (22.21), 203 (100). Anal. Calcd. for C₂₆H₂₁N₅O₄S₂ (531.61): C, 57.74; H, 3.98; N, 13.17. Found: C, 57.46; H, 3.77; N, 12.84.

4.1.2.15. (*Z*)-*N*-(2,6-Dimethoxypyrimidin-4-yl)-4-(3-oxo-3-(10*H*-phenothiazine-2-yl) prop-1-enyl-amino) benzenesulfonamide (**19**). Yield, 80%; m.p. 199.4 °C. IR: 3311, 3166 (NH), 3072 (arom.), 2949, 2899 (aliph.), 1637 (CO), 1589 (CN), 1363, 1155 (SO₂). ¹H NMR: 3.6, 3.7 (2s, 6H, 2OCH₃), 5.9 (s, 1H, CH pyrimidine), 6.1, 7.5 (2d, 2H, CH=CH, *J* = 10 Hz), 6.7–7.4 (m, 11H, Ar-H), 8.5 (s, 1H, SO₂NH), 10.4

(s, 1H, NH phenothiazine), 11.9 (s, 1H, NH). ^{13}C NMR: 54.2, 55.0, 84.9, 95.5, 112.7, 112.9 (2), 113.0, 115.0, 115.8, 116.5, 121.5, 126.3, 126.5, 128.7, 129.6, 129.7, 129.8 (2), 141.7, 142.5 (2), 143.3, 160.3, 164.7, 172.5, 187.2. MS m/z (%): 561 (M^+) (15.31), 77 (100). Anal. Calcd. for $\text{C}_{27}\text{H}_{23}\text{N}_5\text{O}_5\text{S}_2$ (561.63): C, 57.74; H, 4.13; N, 12.47. Found: C, 57.96; H, 4.39; N, 12.81.

4.1.2.16. (Z)-N-(5,6-Dimethoxypyrimidin-4-yl)-4-(3-oxo-3-(10H-phenothiazine-2-yl) prop-1-enyl-amino) benzenesulfonamide (**20**). Yield, 78%; m.p. 141.2 °C. IR: 3377, 3300 (NH), 3062 (arom.), 2945, 2861 (aliph.), 1635 (CO), 1583 (CN), 1373, 1159 (SO_2). ^1H NMR: 3.7, 3.8 (2s, 6H, 2OCH₃), 6.0, 7.5 (2d, 2H, CH=CH, $J = 10$ Hz), 6.6–7.4 (m, 11H, Ar-H), 8.1 (s, 1H, CH pyrimidine), 8.8 (s, 1H, SO_2NH), 10.4 (s, 1H, NH phenothiazine), 11.9 (s, 1H, NH). ^{13}C NMR: 54.5, 60.6, 95.4, 112.6, 112.7 (2), 113.0, 115.2, 115.9, 116.2, 122.0, 126.5, 126.7, 127.7, 128.3, 129.9, 130.1 (2), 133.5, 141.7, 142.5 (2), 143.4, 150.9, 162.0, 172.2, 187.1. MS m/z (%): 561 (M^+) (10.26), 93 (100). Anal. Calcd. for $\text{C}_{27}\text{H}_{23}\text{N}_5\text{O}_5\text{S}_2$ (561.63): C, 57.74; H, 4.13; N, 12.47. Found: C, 58.11; H, 4.38; N, 12.85.

4.1.2.17. (Z)-N-(1H-Indazol-6-yl)-4-(3-oxo-3-(10H-phenothiazine-2-yl) prop-1-enylamino) benzenesulfonamide (**21**). Yield, 85%; m.p. 259.3 °C. IR: 3385, 4342 (NH), 3066 (arom.), 2966, 2841 (aliph.), 1635 (CO), 1591 (CN), 1348, 1186 (SO_2). ^1H NMR: 6.0, 7.4 (2d, 2H, CH=CH, $J = 10.5$ Hz), 6.5–7.3 (m, 15H, Ar-H + CH indazole), 8.7 (s, 1H, SO_2NH), 10.3 (s, 1H, NH phenothiazine), 11.9 (s, 1H, NH), 12.8 (s, 1H, NH indazole). ^{13}C NMR: 91.0, 95.4, 112.7 (2), 113.1 (2), 113.2, 115.0, 115.3, 115.9, 116.5, 120.2, 121.5, 122.5, 126.5, 128.2, 129.0, 129.2, 133.4 (2), 136.6, 140.7, 142.1 (2), 143.3, 144.3, 145.3, 187.1. MS m/z (%): 539 (M^+) (6.81), 181 (100). Anal. Calcd. for $\text{C}_{28}\text{H}_{21}\text{N}_5\text{O}_3\text{S}_2$ (539.63): C, 62.32; H, 3.92; N, 12.98. Found: C, 62.53; H, 4.28; N, 13.33.

4.1.2.18. (Z)-4-(3-Oxo-3-(10H-phenothiazine-2-yl) prop-1-enylamino)-N-(quinoxalin-2-yl) benzenesulfonamide (**22**). Yield, 78%; m.p. 231.5 °C. IR: 3439, 3360 (NH), 3072 (arom.), 2979, 2841 (aliph.), 1635 (CO), 1591 (CN), 1346, 1190 (SO_2). ^1H NMR: 5.9, 7.5 (2d, 2H, CH=CH, $J = 10$ Hz), 6.7–7.3 (m, 16H, Ar-H), 8.7 (s, 1H, SO_2NH), 10.4 (s, 1H, NH phenothiazine), 11.9 (s, 1H, NH). ^{13}C NMR: 95.4, 112.7, 113.0 (2), 114.9, 115.0, 115.8, 116.3, 120.4, 121.4, 122.4, 126.1, 126.5, 127.5, 128.2, 128.3, 129.1, 130.2, 130.5 (2), 131.1, 131.3, 138.8, 141.8, 142.1 (2), 146.7, 160.0, 185.1. MS m/z (%): 551 (M^+) (16.70), 193 (100). Anal. Calcd. for $\text{C}_{29}\text{H}_{21}\text{N}_5\text{O}_3\text{S}_2$ (551.64): C, 63.14; H, 3.84; N, 12.70. Found: C, 63.50; H, 3.93; N, 12.98.

4.1.3. (Z)-3-(4-Aminophenylsulfonyl) phenylamino)-1-(10H-phenothiazin-2-yl)prop-2-en-1-one (**24**)

A mixture of **3** (2.96 g, 0.01 mol) and dapson **23** (2.48 g, 0.01 mol) in absolute ethanol (10 mL) and glacial acetic acid (5 mL) was refluxed for 13 h. The obtained solid was crystallized from dioxane to give **24**.

Yield, 80%; m.p. 317.1 °C. IR: 3356, 3213, 3153 (NH_2 , NH), 3057 (arom.), 2941, 2861 (aliph.), 1635 (CO), 1363, 1197 (SO_2). ^1H NMR: 6.1, 7.5 (2d, 2H, CH=CH, $J = 10.5$ Hz), 6.2 (s, 2H, NH_2), 6.5–7.4 (m, 15H, Ar-H), 10.4 (s, 1H, NH phenothiazine), 11.9 (s, 1H, NH). ^{13}C NMR: 95.3, 112.7, 113.0 (2), 113.4 (2), 115.0, 115.8, 115.9, 116.8, 121.4, 126.5, 126.7, 128.1, 129.5 (4), 129.6, 129.7 (2), 141.7, 141.8 (2), 144.8, 153.8, 187.0. MS m/z (%): 499 (M^+) (1.83), 483 (100). Anal. Calcd. for $\text{C}_{27}\text{H}_{21}\text{N}_3\text{O}_3\text{S}_2$ (499.60): C, 64.91; H, 4.24; N, 8.41. Found: C, 64.59; H, 4.09; N, 8.14.

4.1.4. (Z,Z')-3, 3'-(4,4'-sulfonylbis(4,1-phenylene)bis(azanediyl)) bis(1-(10H-phenothiazin-2-yl) prop-2-en-1-one) (**25**)

A mixture of **3** (5.92 g, 0.02 mol) and dapson **23** (2.48 g, 0.01 mol) in absolute ethanol (20 mL) and glacial acetic acid (5 mL)

was refluxed for 18 h. The obtained solid was crystallized from acetic acid to give **25**.

Yield, 79%; m.p. 233.3 °C. IR: 3410, 3354 (NH), 3055 (arom.), 2917, 2880 (aliph.), 1635 (2CO), 1390, 1197 (SO_2). ^1H NMR: 5.7, 7.4 (2d, 4H, 2CH = CH, $J = 12.5$ Hz), 6.6–7.3 (m, 22H, Ar-H), 10.4 (s, 2H, 2NH phenothiazine), 11.9 (s, 2H, 2NH). ^{13}C NMR: 95.3 (2), 112.7 (2), 113.0 (4), 113.4 (2), 114.9 (2), 115.0 (2), 116.8 (2), 121.5 (2), 126.5 (2), 126.7 (2), 128.2 (2), 128.8 (6), 129.7 (2), 141.8 (2), 143.3 (4), 145.1 (2), 185.1 (2). MS m/z (%): 750 (M^+) (49.8), 374 (100). Anal. Calcd. for $\text{C}_{42}\text{H}_{30}\text{N}_4\text{O}_4\text{S}_3$ (750.91): C, 67.18; H, 4.03; N, 7.46. Found: C, 67.48; H, 4.32; N, 7.77.

4.2. Biological evaluation

4.2.1. SRB cytotoxicity assay

T47D breast cancer cells (obtained from National Cancer Institute, Cairo, Egypt) and 184A1 normal breast cells (obtained from VACSERA, Cairo, Egypt) were grown in RPMI-1640 medium supplemented with 5% heat-inactivated fetal calf serum (FCS), 1 mmol L^{-1} L-glutamine, and 50 $\mu\text{g mL}^{-1}$ gentamicin and maintained at 37 °C in a humidified atmosphere containing 5% CO_2 . The cells were maintained as “monolayer culture” by serial subculturing. Exponentially growing cells were collected using 0.25% Trypsin-EDTA and seeded in 96-well plates at 1000–2000 cells/well in RPMI-1640 supplemented medium. After 24 h, cells were incubated for 48 h with various concentrations (5, 12, 25 and 50 $\mu\text{mol L}^{-1}$) of the tested compounds. Following 48 h treatment, the cells will be fixed with 10% trichloroacetic acid for 1 h at 4 °C. Wells were stained for 30 min at room temperature with 0.4% SRB dissolved in 1% acetic acid. The plates were air dried for 24 h and the dye was solubilized with Tris-HCl for 5 min on a shaker at 1600 rpm. The optical density (OD) of each well was measured spectrophotometrically at 564 nm with an ELISA microplate reader (ChromoMate-4300, FL, USA). The IC_{50} values were calculated according to the equation for Boltzmann sigmoidal concentration–response curve using the nonlinear regression fitting models (Graph Pad, Prism Version 5) [17].

4.2.2. Aromatase assay

Aromatase activity and IC_{50} of the selected compounds were determined in T47D cells which were obtained from American Type Culture Collection, T47D cells were cultured using DMEM (Invitrogen/Life Technologies) supplemented with 10% FBS (Hyclone), 10 $\mu\text{g/ml}$ of insulin (Sigma), and 1% penicillin-streptomycin. All the other chemicals and reagents were from Sigma, or Invitrogen. Plate cells (cells density $1.2\text{--}1.8 \times 10,000$ cells/well) in a volume of 100 μl complete growth medium + 100 μl of the tested compound per well in a 96-well plate for 18–24 h before the enzyme assay for aromatase. T47D cells were treated with serial dilutions of the selected potent compounds for 24 h and then the aromatase activity was determined as previously mentioned.

4.2.3. Effect on active caspase-3

The active caspase-3 level was measured by using Quantikine –Human active Caspase-3 Immunoassay (R&D Systems, Inc. Minneapolis, USA) according to the manufacturer protocol by a method developed in our lab.

4.2.4. Effect on caspase-8 & caspase-9

Human caspase-8 ELISA kit (EIA-4863) and human caspase-9 ELISA kit DRG[®] Caspase-9 (EIA-4860) (DRG International Inc., USA) were used, and the procedure adopted by our lab.

4.2.5. PCR analysis and quantification of gene expression of BAX, Bcl-2, Bcl-X_L

RNeasy Mini Kit[®] (Qiagen Inc. Valencia, CA, USA) was used for the total RNA extraction from cells. Reverse transcription was undertaken to construct cDNA library from different treatments using High-Capacity cDNA Reverse Transcription Kit (Applied Biosystems, Foster City, CA). The archived cDNA libraries were then subjected to quantitative real-time PCR reactions using cyber green fluorophore (Fermentas Inc., Glen Burnie, MD, USA). Primer sequences were as follows: Bcl-2 forward primer GGG-TAC-GAT-AAC-CGG-GAG-AT and reverse primer CTG-AAG-AGC-TCC-TCC-ACC-AC; BAX forward primer TCT-GAC-GGC-AAC-TTC-AAC-TG and reverse primer TGG-GTG-TCC-CAA-AGT-AGG-AG; Bcl-X_L forward primer GGC GGA TTT GAA TCT CTT TCT C and reverse primer TTA TAA TAG GGA TGG GCT CAA CC; reference housekeeping gene used was GAPDH with forward primer TGC-ACC-ACC-AAC-TGC-TTA-G and reverse primer GAT-GCA-GGG-ATG-ATG-TTC.

4.3. Molecular docking

The crystal structure of the aromatase enzyme co-crystallized with the androstenedione (ASD) substrate was obtained from the Protein Data Bank (PDB ID: 3EQM). Docking study was performed using Accelrys software (Discovery Studio 2.5) in the computer drug design lab in the pharmaceutical chemistry department, Faculty of pharmacy, Ain Shams University. The protein was prepared by prepare protein protocol. Our ligands were drawn as a database and prepared by prepared ligand protocol during which it was refined using CHARMM force field with full potential. CDOCKER protocol was then run, and different binding poses were ranked according to the calculated interaction binding energies and the binding mode was analyzed for each compound. Also, ADMET study was performed in the same lab using Accelrys software (Discovery Studio 2.5). Some of the parameters that are calculated using Accord for Excel includes Atom based Log P98 (A LogP 98), ADMET 2D polar surface area (ADMET 2D PSA), Aqueous solubility (AQ SOI), Aqueous solubility level (AQ SOI LEV), Blood Brain Barrier value (BBB), Blood Brain Barrier Level (BBB LEV), Cytochrome P450 2D6 (CYP2D6), Cytochrome P450 2D6 Probability (CYP PROB), Hepatotoxicity Level (HEPATOX LEV), Hepatotoxicity Probability (HEPATOX PROB), Plasma protein binding logarithmic value (PPB LOG) and Plasma protein binding logarithmic level (PPB LEV). The compounds structures were drawn using DS Viewer ProSuite software and appended into Accord for Excel software then the parameters were calculated.

Acknowledgment

The authors are thankful to the Deanship of the Scientific Research and Research Center, College of Pharmacy, King Saud University, Riyadh, Saudi Arabia.

Appendix A. Supplementary data

Supplementary data related to this article can be found at <http://dx.doi.org/10.1016/j.ejmech.2017.04.028>.

References

- [1] T. Rudel, Caspase inhibitors in prevention of apoptosis, *Herz* 24 (1999) 236–241.
- [2] L.-W. Zheng, Y. Li, D. Ge, B.-X. Zhao, Y.-R. Liu, H.-S. Lv, J. Ding, J.-Y. Miao, Synthesis of novel oxime-containing pyrazole derivatives and discovery of regulators for apoptosis and autophagy in A549 lung cancer cells, *Bioorg. Med. Chem. Lett.* 20 (2010) 4766–4770.
- [3] J. Zhang, J.E. Riby, L. Conde, W.E. Grizzle, X. Cui, C.F. Skibola, A Fucus vesiculosus extract inhibits estrogen receptor activation and induces cell death in female cancer cell lines, *BMC Complement. Altern. Med.* 16 (2016) 151–159.
- [4] R.B. Riggins, A.H. Bouton, M.C. Liu, R. Clarke, Antiestrogens, aromatase inhibitors, and apoptosis in breast cancer, *Vitam. Horm.* 71 (2005) 201–237.
- [5] J. Cui, Y. Shen, R. Li, Estrogen synthesis and signaling pathways during aging: from periphery to brain, *Trends Mol. Med.* 19 (2013) 197–209.
- [6] S. Yahiaoui, C. Fagnere, C. Pouget, J. Buxeraud, A.-J. Chulia, New 7,8-benzoflavanones as potent aromatase inhibitors: synthesis and biological evaluation, *Bioorg. Med. Chem.* 16 (2008) 1474–1480.
- [7] L.A. Hasvold, W. Wang, S.L. Gwaltney, T.W. Rockway, L.T. Nelson, R.A. Mantei, S.A. Fakhoury, G.M. Sullivan, Q. Li, N.-H. Lin, Pyridone-Containing farnesyltransferase inhibitors: synthesis and biological evaluation, *Bioorg. Med. Chem. Lett.* 13 (2003) 4001–4005.
- [8] S. Anusha, C.D. Mohan, H. Ananda, C.P. Baburajeev, S. Rangappa, J. Mathai, J.E. Fuchs, F. Li, M.K. Shanmugam, A. Bender, G. Sethi, Basappa, K.S. Rangappa, Adamantyl-tethered-biphenylic compounds induce apoptosis in cancer cells by targeting Bcl homologs, *Bioorg. Med. Chem. Lett.* 26 (2016) 1056–1060.
- [9] I. Ahmad, Shagufta, Recent developments in steroidal and nonsteroidal aromatase inhibitors for the chemoprevention of estrogen-dependent breast cancer, *Eur. J. Med. Chem.* 102 (2015) 375–386.
- [10] W. Lv, J. Liu, D. Lu, D.A. Flockhart, M. Cushman, Synthesis of mixed (E,Z)-, (E)-, and (Z)-Norendoxifen with dual aromatase inhibitory and estrogen receptor modulatory activities, *J. Med. Chem.* 56 (2013) 4611–4618.
- [11] M.M. Ghorab, M.S. Alsaied, G.H. Al-Ansary, G.A. Abdel-Latif, D.A. Abou El Ella, Analogue based drug design, synthesis, molecular docking and anticancer evaluation of novel chromene sulfonamide hybrids as aromatase inhibitors and apoptosis enhancers, *Eur. J. Med. Chem.* 124 (2016) 946–958.
- [12] R. Pingaew, V. Prachayasittikul, P. Mandi, C. Nantasenamat, S. Prachayasittikul, S. Ruchirawat, V. Prachayasittikul, Synthesis and molecular docking of 1,2,3-triazole-based sulfonamides as aromatase inhibitors, *Bioorg. Med. Chem.* 23 (2015) 3472–3480.
- [13] D.A.A. El Ella, M.M. Ghorab, H.I. Heiba, A.M. Soliman, Synthesis of some new thiazolopyrane and thiazolopyranopyrimidine derivatives bearing a sulfonamide moiety for evaluation as anticancer and radiosensitizing agents, *Med. Chem. Res.* 2 (2012) 2395–2407.
- [14] M.M. Ghorab, F.A. Ragab, H.I. Heiba, A.M. Soliman, Design and synthesis of some novel 4-Chloro-N-(4-(1-(2-(2-cyanoacetyl) hydrazono) ethyl) phenyl) benzenesulfonamide derivatives as anticancer and radiosensitizing agents, *Eur. J. Med. Chem.* 117 (2016) 8–18.
- [15] J. Jenkins, *Workbook for Organic Chemistry*, Macmillan, 2009.
- [16] M.S. Al-Said, M.M. Ghorab, Y.M. Nissan, Dapson in heterocyclic chemistry, part VIII: synthesis, molecular docking and anticancer activity of some novel sulfonylbiscompounds carrying biologically active 1, 3-dihydropyridine, chromene and chromenopyridine moieties, *Chem. Cent. J.* 6 (2012) 64–77.
- [17] P. Skehan, R. Storeng, D. Scudiero, A. Monks, J. McMahon, D. Vistica, J.T. Warren, H. Bokesch, S. Kenney, M.R. Boyd, New colorimetric cytotoxicity assay for anticancer-drug screening, *J. Natl. Cancer Inst.* 82 (1990) 1107–1112.
- [18] S.J. Martin, Caspases: executioners of apoptosis, *Pathobiol. Hum. Dis.* (2014) 145–152.
- [19] S. Fulda, L. Galluzzi, G. Kroemer, Targeting mitochondria for cancer therapy, *Nat. Rev.* 9 (2010) 447–464.
- [20] S. Salakou, D. Kardamakis, A.C. Tsamandas, V. Zolota, E. Apostolakis, V. Tzelepi, P. Papathanasopoulos, D.S. Bonikos, T. Papapetropoulos, T. Petsas, D. Dougenis, Increased Bax/Bcl-2 ratio up-regulates caspase-3 and increases apoptosis in the thymus of patients with myasthenia gravis, *In Vivo (Athens, Greece)* 21 (2007) 123–132.
- [21] C. Vignon, C. Debeissat, M.-T. Georget, D. Bouscary, E. Gyan, P. Rosset, O. Herault, Flow cytometric quantification of all phases of the cell cycle and apoptosis in a two-color fluorescence plot, *PLoS One* 8 (2013) e68425.
- [22] M. Chi, H. Evans, J. Gilchrist, J. Mayhew, A. Hoffman, E.A. Pearsall, H. Jankowski, J.S. Brzozowski, K.A. Skelding, Phosphorylation of calcium/calmodulin-stimulated protein kinase II at T286 enhances invasion and migration of human breast cancer cells, *Sci. Rep.* 6 (2016) 33132.
- [23] D. Ghosh, J. Griswold, M. Erman, W. Pangborn, Structural basis for androgen specificity and oestrogen synthesis in human aromatase, *Nature* 457 (2009) 219–223.